WBF/GF HH resonances from a phenomenological perspective

Rahool Kumar Barman
Indian Association for the Cultivation of Science

based on: **JHEP 1909 (2019) 068** (with A. Adhikary (IISc Bangalore), S.Banerjee (CERN) and B. Bhattacherjee (IISc))
and
Phys. Rev. D 102, 055014 (with C. Englert (Univ. of Glasgow), D. Goncalves (Oklahoma State Univ.), M. Spannowsky (IPPP Durham))

Higgs 2020

October 27, 2020

Outline

1. Introduction
2. Resonant di-Higgs searches in gluon fusion at the HL-LHC and its implications on pMSSM
3. Di-Higgs resonant searches in weak boson fusion

Introduction

- The ATLAS and CMS collaborations have unambiguously confirmed the existence of a scalar boson at 125 GeV.
- Numerous studies performed to measure the coupling of the Higgs boson with the SM particles.
- Significant deviations from the SM expectation have remained mostly elusive.
- Our understanding of the fundamental nature of the electroweak symmetry breaking (EWSB) is also lacking.
- Measurement of the elusive Higgs self-coupling (λ) is essential to the understanding of the EWSB picture.
- In the SM, double Higgs and triple Higgs production are the only direct probes for λ.
- However, the experimental investigations of multi-Higgs states suffer from low statistics.

Non-resonant di-Higgs searches

Gluon-fusion (GF) mode in SM

- Contributes to $\gtrsim 90\%$ of the total NR hh cross-section at the LHC.
- Destructive interference between the triangle and the box diagram leads to a small cross-section, ~ 33 fb at $\sqrt{s} = 13$ TeV.

VBF mode in SM

- Very small cross-section at 13 TeV LHC:~ 1.73 fb.
- Sensitive to both λ as well as c_{2V}.

The small cross-section makes it extremely challenging to probe di-Higgs production at the current LHC.

However, phenomenologically rich final states can emerge:

hh $\rightarrow$ 4b (33 %), 2b2W (25 %), 2b2τ (7 %), 2b2γ (10^{-3})

Limits from non-resonant *hh* searches

- ATLAS: 13.3 fb^{-1}: 4b: $\sim$ 29 times
- ATLAS: 36.1 fb^{-1}: $2b2\tau$: $\sim$ 13 times
- CMS: 35.9 fb^{-1}: $2b2\gamma$: $\sim$ 30 times
- CMS: 35.9 fb^{-1}: $2b2\gamma$: $\sim$ 19 times

- An enhancement in the *hh* cross-section could make the channel noticeable.

Various new physics scenarios can lead to such an enhancement.

Non-resonant enhancement:

- Deviations from $\lambda_{SM} \to$ can modify the GF as well as the WBF *hh* production rates.
- Deviations in $c_{2v} \to$ can significantly increase the WBF *hh* cross-section. [1]

Resonant enhancement:

- BSM theories consisting of new particles which can decay to *hh* $\to$ enhance the detectability of both GF and WBF *hh* modes.
- Heavy Higgs states in well-motivated BSM scenarios: MSSM, NMSSM, singlet-extensions, etc.

[1] Eur.Phys.J. C **77** 481 (2017)

Status of (non-) resonant di-Higgs searches

$\sqrt{s} = 13$ TeV, $\mathcal{L} \sim 36$ fb^{-1}

Channel	CMS (NR) ($\times$SM)	CMS (R) [fb, (GeV)]	ATLAS (NR) ($\times$SM)	ATLAS (R) [fb, (GeV)]
$b\bar{b}b\bar{b}$	75	1500 – 45 (260 – 1200)	13	2000 – 2 (260 – 3000)
$b\bar{b}\gamma\gamma$	24	240 – 290 (250 – 900)	19.2	1100 – 120 (260 – 1000)
$b\bar{b}\tau^+\tau^-$	30	3110 – 70 (250 – 900)	12.7	1780 – 100 (260 – 1000)
$\gamma\gamma WW^*$ ($\gamma\gamma\ell\nu jj$)			200	40000 – 6100 (260 – 500)
$b\bar{b}\ell\nu\ell\nu$	79	20500 – 800 (300 – 900)	300	6000 – 170 (500 – 3000)
WW^*WW^*			160	9300 – 2800 (260 – 500)

Mass range, Upper limit, NR: non-resonant, R: resonant.

Resonant hh production in GF mode at the HL-LHC

- The case of $H \to hh \to 2b2\gamma$ is discussed, where H is produced through the GF mode.
- The high reconstruction and identification precision of the photons at the LHC compensates for the small $h \to \gamma\gamma$ branching rate.

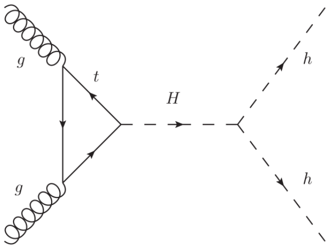

Backgrounds

- $hh + X$: SM di-Higgs production.
- $h + X$: Zh, $hb\bar{b}$, $t\bar{t}h$.
- Null Higgs: $b\bar{b}\gamma\gamma$, $t\bar{t} + t\bar{t}\gamma$ (leptons may fake as γ), $c\bar{c}\gamma\gamma + jj\gamma\gamma$ (light *jets* fake as *b-jets*), $b\bar{b}j\gamma + c\bar{c}j\gamma$ (Fake 1), $b\bar{b}jj$ (Fake 2).
- Single Higgs production: $hjj + hc\bar{c}$.

Signal generation: `Pythia-6`, Background generation: `MG5_aMC@NLO` + `Pythia-6`, Detector simulation: `Delphes-3.4.1`

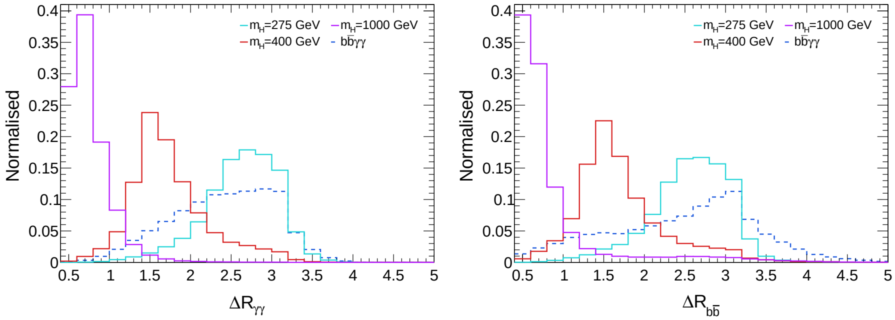

$$122\ \text{GeV} < m_{\gamma\gamma} < 128\ \text{GeV}$$
$$N_b = 2,\ N_\gamma = 2,\ N_\ell = 0$$
$$p_{T,b} > 40\ (30)\ \text{GeV},\ \ p_{T,\gamma} > 30\ (30)\ \text{GeV}$$
$$0.4 < \Delta R_{\gamma\gamma} < (3.0/2.0/1.5),\ 0.4 < \Delta R_{bb} < (3.0/2.0/1.5),$$
$$(m_H = 275\text{-}350\ \text{GeV}/400\text{-}600\ \text{GeV}/0.8\text{-}1\ \text{TeV})$$
$$\Delta R_{\gamma b} > 0.4,\ 90\ \text{GeV} < m_{bb} < 130\ \text{GeV}$$

Applied cuts

Signal efficiency

The cuts on $m_{bb\gamma\gamma}$ and $p_{T,\gamma\gamma}$ are also optimized.

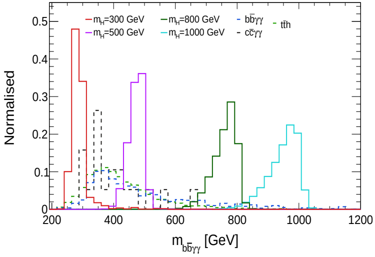

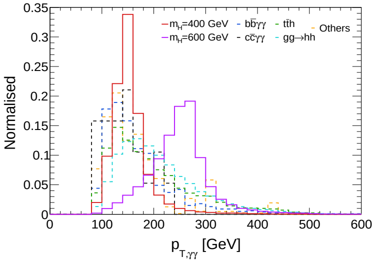

Optimized cuts along with the signal efficiency and the background yields.

Heavy Higgs mass, m_H (GeV)	Optimised cuts		After all cuts	
	$m_{b\bar{b}\gamma\gamma}$ (GeV)	$p_{T,\gamma\gamma} >$ (GeV)	Signal Efficiency (ϵ)	Background yield at 3000 fb^{-1}
275	[235 , 275]	50	0.012	30.01
350	[300 , 355]	100	0.024	23.33
500	[445 , 510]	100	0.051	10.87
600	[460 , 615]	100	0.076	18.11
800	[560 , 830]	100	0.091	9.54
1000	[780 , 1030]	100	0.090	2.31

Projected upper limits

- Projected UL on $\sigma(pp \to H \to hh)$ as a function of m_H for the $b\bar{b}\gamma\gamma$ channel at the HL-LHC.
- The results from our multivariate analysis are also comparable to the cut-based analysis.

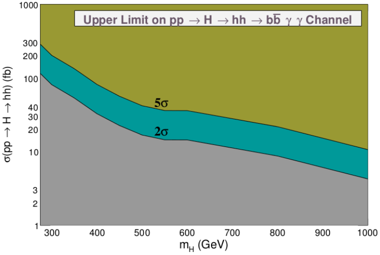

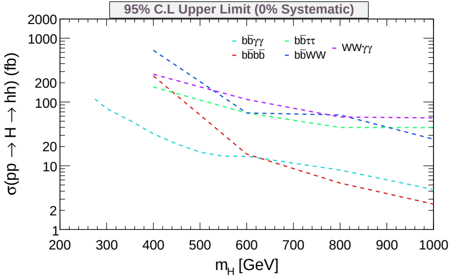

- $b\bar{b}\gamma\gamma$ is strongest upto $m_H \sim 600$ GeV.
- Above 600 GeV, $4b$ is more constraining.
- The HL-LHC projections are roughly an order of magnitude improved than the present upper limits.
- Roughly an order of magnitude stronger than the current limits.

Implications on pMSSM

The parameter space:

$$
\begin{aligned}
1 < \tan\beta < 60,\ 200\ \text{GeV} < m_A < 1\ \text{TeV},\ 1\ \text{TeV} < M_3 < 10\ \text{TeV} \\
1\ \text{TeV}\ <\ M_{\tilde{Q}_3,\tilde{u}_3,\tilde{d}_3}\ <\ 20\ \text{TeV},\ -10\ \text{TeV} < A_{t,b} < 10\ \text{TeV} \\
1\ \text{TeV}\ <\ M_{\tilde{Q}_1,\tilde{u}_1,\tilde{d}_1}\ <\ 20\ \text{TeV},\ M_{\tilde{Q}_2} = M_{\tilde{Q}_1}, M_{\tilde{u}_2} = M_{\tilde{u}_1}, M_{\tilde{d}_2} = M_{\tilde{d}_1} \\
A_{e,\mu,\tau,u,d,c,s} = 0,\ M_{\tilde{e}_{1_L},\tilde{e}_{1_R},\tilde{e}_{2_L},\tilde{e}_{2_R},\tilde{e}_{3_L},\tilde{e}_{3_R}}\ =\ 3\ \text{TeV},\ 600\ \text{GeV}\ <\ M_{1,2},\mu\ <\ 5\ \text{TeV}
\end{aligned}
\tag{1}
$$

- The GF channel is the dominant Higgs production mode at low values of $\tan\beta$.
- The $H \to hh$ decay mode also gains dominance in the low and intermediate $\tan\beta$ regime.
- The current search limits on $H \to hh$ do not impose any constraints on the parameter space.
- Constraints from $\sigma_{b\bar{b}H/A} \times Br(H/A \to \tau\tau)$ exclude the low m_A and high $\tan\beta$ regions.)
- We translate the HL-LHC projections onto the pMSSM parameter space.

Implications on pMSSM

- Grey points $\rightarrow$ excluded by the upper limits on $\sigma_{b\bar{b}H/A} \times Br(H/A \rightarrow \tau\tau)$ derived by ATLAS and CMS ($\mathcal{L} \sim 36\ \mathrm{fb}^{-1}$).
- Red points: Within the projected reach of the $gg \rightarrow H \rightarrow hh \rightarrow b\bar{b}\gamma\gamma$ search channel at the HL-LHC.
- Green points: Within the projected reach of $gg \rightarrow H \rightarrow t\bar{t}$.
- Blue points: **Would remain allowed after the HL-LHC run.**

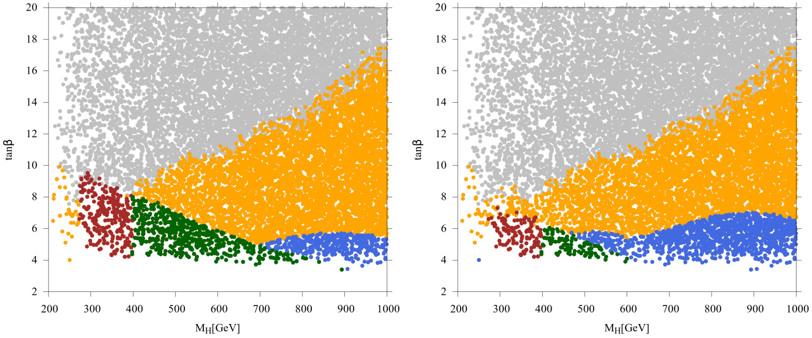

Left panel: 2σ, Right panel: 5σ

Resonant hh production via WBF mode at the HL-LHC

- WBF production becomes more pertinent in scenarios with singlet-like Higgs states at $\sim O\,(\mathrm{TeV})$ where the GF and WBF productions become comparable.
- In such cases, it is expected that both the WBF and GF signals would play an important role in the discovery of new physics.

A typical example $\rightarrow$ NMSSM with a dominantly singlet-like heavy Higgs.
[Phys. Rev. D **99**, 095035]

- Searches in the $H \rightarrow t\bar{t}$ mode might impart a smaller sensitivity due to the accidental destructive interference with the QCD continuum $t\bar{t}$ production $\longrightarrow$ in such a case, $H \rightarrow hh$ could be the only phenomenologically robust search mode.

The model

The SM Higgs doublet (Φ_{SM}) is extended with an additional singlet (Φ_s) under the SM gauge group.

$$V = \mu_s^2|\Phi_s|^2 + \lambda_s|\Phi_s|^4 + \mu_h^2|\Phi_h|^2 + \lambda_h|\Phi_h|^4 + \eta|\Phi_s|^2|\Phi_h|^2$$

With Φ_i defined as $(v_i + H_i)/\sqrt{2}$, the Higgs mass eigenstates can be expressed as:

$$\begin{aligned} h &= \quad \cos\theta\, H_{SM} + \sin\theta\, H_S \\ H &= -\sin\theta\, H_{SM} + \cos\theta\, H_S\,. \end{aligned} \tag{2}$$

h is is identified with the SM 125 GeV Higgs boson.

- Compared to SM, the signal strength of h gets modified by $\cos^2\theta$.
- For $m_H \leq 2m_h$, $\sigma(pp \to H) = \sin^2\theta\ \sigma(pp \to h)_{m_h=m_H}$.
- We consider the case where $m_H > 2m_h$.

The WBF channel

We focus on WBF Higgs pair production via: $pp \to Hjj \to (hh \to 4b)jj$.

- This final state benefits from the improved signal yield due to the large $h \to b\bar{b}$ branching ratio.
- This final state also suffers from a large multijet background.
- However, the characteristic VBF topology helps in efficiently discriminating the signal from the background.
- The VBF topology features two forward *jets* well separated by rapidity.
- These forward *jets* also feature a large invariant mass.
- Reduced hadronic activity in the central region.
- The lighter Higgs bosons can acquires a considerable boost.

The WBF channel

- VBF signal generation: $pp \to Hjj \to (H \to hh \to 4b)\, jj$, with VBFNLO.
- The dominant backgrounds are: $4b + 2j$, $2b + 4j$ and $t\bar{t}b\bar{b}$.
- Backgrounds are generated at LO with MadGraph5_aMC@NLO; Showering and hadronization simulated with Pythia-8.
- *Jets* defined with anti-k_t algorithm: $\mathrm{R} = 0.4$, $p_{T_j} > 30$ GeV, $|\eta_j| < 4.5$. using FastJet.
- b-tagging efficiency is assumed to be 70%.

The entire analysis can be sub-divided into three categories:

1. Basic selection.
2. Identification of WBF topology.
3. Higgs boson reconstruction.

The WBF channel

- VBF signal generation: $pp \to Hjj \to (H \to hh \to 4b)\, jj$, with `VBFNLO`.
- The dominant backgrounds are: $4b + 2j$, $2b + 4j$ and $t\bar{t}b\bar{b}$.
- Backgrounds are generated at LO with MadGraph5_aMC@NLO; Showering and hadronization simulated with `Pythia-8`.
- *Jets* defined with anti-k_t algorithm: $\mathrm{R} = 0.4$, $p_{T_j} > 30$ GeV, $|\eta_j| < 4.5$. using `FastJet`.
- *b*-tagging efficiency is assumed to be 70%.

The entire analysis can be sub-divided into three categories:

1. Basic selection.

- $N_j \geq 6$, $N_{b-jets} = 4$.
- Veto leptons with $p_t > 12$ GeV and $|\eta| < 2.5$.
- Invariant mass of the 4 *b-jets*, $m_{4b} > 350$ GeV.

The WBF topology

The WBF topology is identified through:

- Two light-flavored highest rapidity *jets* falling in different hemispheres: $\eta_{j_1}\eta_{j_2} < 0$.
- Large rapidity separation: $|\eta_{j_1} - \eta_{j_2}| > 4.2$.

The WBF signal is also characterized by a large $m_{j_1 j_2}$:

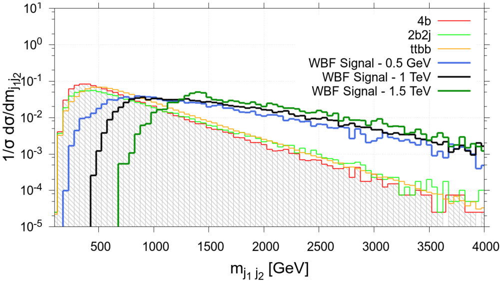

- We also demand: $m_{j_1 j_2} > 1\ \mathrm{TeV}$.

The WBF topology

- The WBF signal displays suppressed *jet* emissions in the central region.
- However, the bulk of the QCD background is centred around the central region.
- Furthermore, the more massive the resonance, the further forward the tagging *jets*.

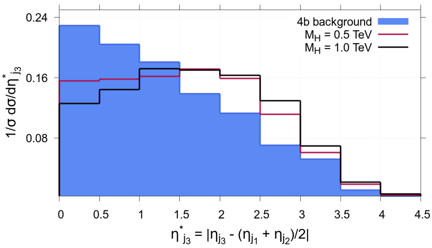

Therefore, we also impose:

$$\left|\eta_{j3} - \frac{\eta_{j1} + \eta_{j2}}{2}\right| > 2.5$$

Higgs reconstruction

Higgs boson reconstruction

1. The *b-jet* pairs with invariant mass closest to 125 GeV is identified with h_1 (the other pair with h_2).
2. The signal region is defined to be within the circular region:

$$\sqrt{\left(\frac{m_{h1} - 125\ \mathrm{GeV}}{20\ \mathrm{GeV}}\right)^2 + \left(\frac{m_{h2} - 125\ \mathrm{GeV}}{20\ \mathrm{GeV}}\right)^2} < 1 \qquad (3)$$

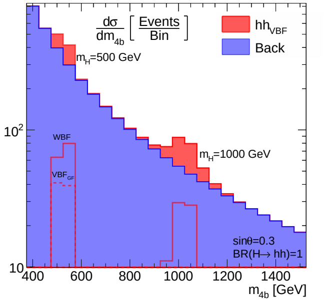

- The stacked m_{4b} distribution is shown.
- The solid red line represents the individual WBF component.
- The dashed red line represents the VBF GF component.
- The reconstructed Higgs boson's four-momentum has been scaled with $m_h/m_{1(2)}$.

Cut-flow table

- Dominant contribution to the signal arises from the WBF component.
- The VBF GF signal also contributes non-negligibly.
- Larger $m_H \rightarrow$ relatively larger contribution from WBF.

Cross-section (in fb) at $\sqrt{s} = 13$ TeV

	Basic selections	VBF topology	Double Higgs reconstruction
WBF $m_H = 500$ GeV	2.6×10^{-1}	1.3×10^{-1}	5.0×10^{-2}
GF $m_H = 500$ GeV	2.2×10^{-1}	7.1×10^{-2}	2.8×10^{-2}
WBF $m_H = 1$ TeV	9.4×10^{-2}	5.4×10^{-2}	3.2×10^{-2}
GF $m_H = 1$ TeV	2.2×10^{-2}	8.3×10^{-3}	4.7×10^{-3}
$4b$	250	47	1.2
$2b2j$	4.9×10^{-1}	1.0×10^{-1}	-
$t\bar{t}b\bar{b}$	90	3.7	3.0×10^{-3}

The 95% C.L. sensitivity to $\sin\theta$ as a function of m_H, for $\sqrt{s} = 13$ GeV LHC at $\mathcal{L} = 3000\ \mathrm{fb}^{-1}$.

- Red-dashed: WBF signal only
- Red-solid: WBF + GF signals.
- **Black**: GF signal only, derived from the CMS $pp \to H \to hh \to 4b$ study [JHEP08 (2018) 152] through scaling with the integrated luminosity.

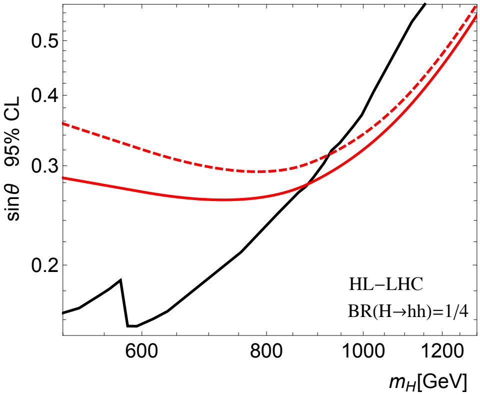

- The VBF GF component contributes non-negligibly in the low mass regime, $500\ \mathrm{GeV} \lesssim m_H \lesssim 900\ \mathrm{GeV}$.
- The WBF search displays stronger limits in the high $m_H \gtrsim 900\ \mathrm{GeV}$ regime.

Implications on the singlet-extension scenario

The VBF and GF limits are interpreted on the singlet-extension model discussed earlier.

Blue points: projected reach from GF signal.

Orange color: projected reach of $pp \to hhjj$ signal.

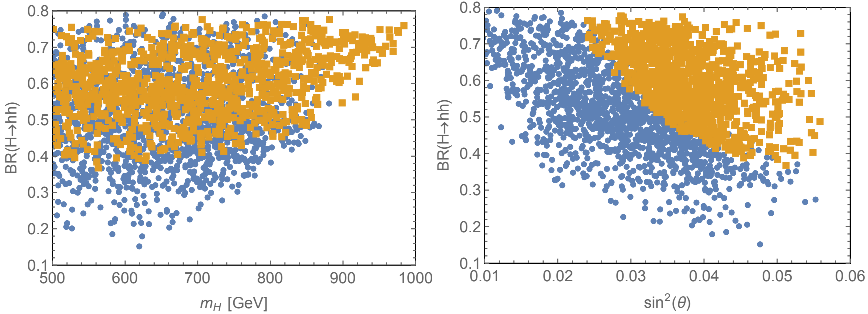

- The VBF provides significant sensitivity at higher masses where the GF projection becomes insensitive.
- We also observe regions in $br(H \to hh)$ where the VBF provides new sensitivity that cannot be accesses by the GF projection.

Conclusions

- Given that the weak boson fusion production cross-section becomes comparable to the GF cross-section for SM-like production around 1 TeV, the WBF channel is a phenomenologically important channel even at small mixing angles.
- The weak boson fusion provides a unique opportunity to probe new physics scenarios through its distinct phenomenological features.
- In scenarios with isospin singlet-mixing, the $H \to hh$ modes might provide phenomenologically robust signals compared to the more obvious decays into top quarks or massive weak bosons.
- The VBF GF channel remains phenomenologically important and should be rightfully included along with the WBF channel in the signal component.

Thank you.